ResearchGate

See discussions, stats, and author profiles for this publication at: https://www.researchgate.net/publication/231654102

Photophysical Properties and Two-Photon Polymerization Ability of a Nitroalkoxystilbene Derivative

ARTICLE *in* THE JOURNAL OF PHYSICAL CHEMISTRY C · DECEMBER 2009

Impact Factor: 4.77 · DOI: 10.1021/jp9075977

CITATIONS
19

READS
32

7 AUTHORS, INCLUDING:

Jean-Pierre Malval
Université de Haute-Alsace
74 PUBLICATIONS **632** CITATIONS
SEE PROFILE

Hélène Chaumeil
Université de Haute-Alsace
55 PUBLICATIONS **413** CITATIONS
SEE PROFILE

Lavinia Balan
French National Centre for Scientific Resea…
134 PUBLICATIONS **1,212** CITATIONS
SEE PROFILE

Albert Defoin
Université de Haute-Alsace
120 PUBLICATIONS **1,219** CITATIONS
SEE PROFILE

Available from: Hélène Chaumeil
Retrieved on: 26 January 2016

Photophysical Properties and Two-Photon Polymerization Ability of a Nitroalkoxystilbene Derivative

Jean-Pierre Malval,*,† Fabrice Morlet-Savary,† Hélène Chaumeil,‡ Lavinia Balan,† Davy-Louis Versace,† Ming Jin,† and Albert Defoin‡

Département de Photochimie Générale, FRE CNRS 3252, and Laboratoire de Chimie Organique et Bioorganique et Macromoleculaire, FRE CNRS 3253, Université de Haute Alsace, ENSCMu. 3 rue Alfred Werner, 68093 Mulhouse, France

Received: August 6, 2009; Revised Manuscript Received: October 17, 2009

The photophysical behavior of the *trans*-4-propoxy 4′-nitrostilbene (**PNS**) as well as its one- and two-photon polymerization properties are reported. A detailed solvatochromic analysis of the steady-state and time-resolved fluorescence indicates that the locally excited state of **PNS** (LE) undergoes multiple deactivation pathways which are sequentially triggered by the solvent polarity. In low polar solvent, an efficient intersystem crossing (ISC) identified as a $S_1 \rightarrow T_n$ process leads to the population of the lowest triple state from which the trans−cis photoisomerization is mainly proceeding. From ns-laser flash photolysis measurements, it also appears that the T_1 state which exhibits a $n\pi^*$ character can efficiently abstract a hydrogen from aliphatic amines and subsequently produces α-aminoalkyl radicals, highly reactive species for the photoinitiation of free-radical polymerization. As a consequence, **PNS** constitutes a good photoinitiating system. However, the further increase of the solvent polarity opens a new relaxation pathway which populates a highly polar TICT level to the detriment of ISC and trans−cis photoisomerization. A strong increase of the fluorescence quantum yield with a concomitant decrease of the trans−cis photoisomerization one is then observed. At the high end of the solvent-polarity scale, an adding non-radiative deactivation process associated with the twisting of the nitro group leads to a noticeable decrease of the fluorescence process. The photoinduced charge transfer process which largely impacts the photophysical feature of such a D−π−A system also promotes the two-photon absorption properties of **PNS**. The chromophore exhibits a sizable two-photon absorption spectrum in the 700−900 nm region with δ of about 180 ± 15 GM at 750 nm. In conjunction with its photoinitiating properties, the two-photon polymerization ability of **PNS** was finally demonstrated. A systematic comparison with a 2,7 diaminofluorene derivative used as reference for two-photon polymerization confirms the substantial improvement of the two-photon polymerization efficiency.

1. Introduction

Two-photon absorption (2PA) in organic molecules is the subject of considerable research, owing to the number of promising applications such as optical limiting,[1,2] two-photon fluorescence imaging,[3–5] photodynamic therapy,[6] 3D microfabrication, and high-density optical data storage.[7–11] The crossing point of all these applications is the requirement of molecular systems with large 2PA cross sections (δ). Therefore, several design strategies have been developed in order to derive relevant structure/property relationships devoted to the improvement of δ. For instance, linear molecules with a large dipolar or quadrupolar character have attracted attention.[1,12–17] Such molecules imply donor−bridge−acceptor (D−π−A) dipolar chromophores and symmetrical D−π−D or A−π−A quadrupolar molecules. Numerous chromophores have been synthesized with modulating the terminal donor and acceptor substituents or with varying the polarizable π-bridging center[18] (phenylene−vinylene, 2,7-fluorenyl, ethynyl, phenylethynyl). Another fruitful strategy consists in increasing the dimensionality of the molecule with an organization of several donor−π−acceptor chromophores into a multibanched configuration.[19–22] Because of a cooperative interaction among each arm, the resulting 2PA cross section was much greater than the sum of the discrete δ units that constitute the entire octupolar chromophore. The improvement of the 2PA ability should be accompanied with the implementation of other molecular properties in order to address the two-photon active materials for specific applications. In the case of two-photon free-radical polymerization, the introduction of an efficient photoinitiator is necessary.[11,23–28] The photoinitiation rate is strongly dependent on the quantum yield of radical generation combined with a high initiation efficiency of the generated radicals. The α-aminoalkyl radicals, for instance, constitute a class of highly reactive radicals upon addition onto acrylate double bond.[29,30] They can be produced from a hydrogen-abstraction reaction between an aliphatic amine and the lowest triplet state (T_1) of the excited photoinitiator. In this case, the efficiency of the reaction depends both on the intersystem crossing quantum yield (Φ_{ISC}) of the chromophore and on the hydrogen abstractability of the T_1 state. This latter parameter is all the more enhanced as the lowest triplet state[31] exhibits a stronger electronic $n\pi^*$ character. In line with these requirements, we report in this paper a relevant approach based on a D−π−A *trans*-stilbene system (Scheme 1) with a propoxy group as a terminal D component and a nitro substituent which displays a double role as a strong electron-withdrawing group and as an efficient spin-coupling agent promoting the intersystem

* Corrsponding author. Tel: +33 389 33 50 24. Fax: +33 389 33 50 11. E-mail: jean-pierre.malval@uha.fr.
† Département de Photochimie Générale.
‡ Laboratoire de Chimie Organique et Bioorganique et Macromoleculaire.

10.1021/jp9075977 © 2009 American Chemical Society
Published on Web 11/17/2009

SCHEME 1: Molecular Structures of the Chromophores

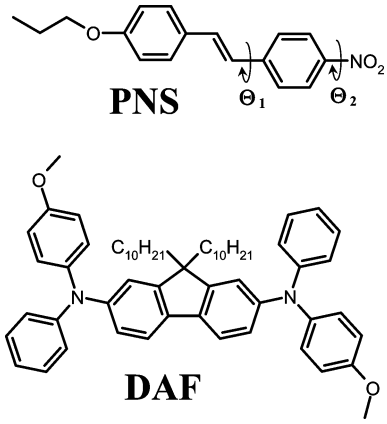

crossing to the triplet manifold. A detailed linear and nonlinear spectroscopic analysis of this push-pull derivative is presented. The two-photon polymerization is investigated by comparison with a 2,7 diaminofluorene derivative used as a reference two-photon initiator (Scheme 1).

2. Experimental Section

2.1. Materials. ***1-(Propoxy)-4-[(E)-2-(4-nitrophenyl)vinyl]-benzene (*PNS*).*** 1-(Propoxy)-4-[(E)-2-(4-nitrophenyl)vinyl]-benzene is obtained in 60% yield by alkylation of a precursor, the 4-[(E)-2-(4-nitrophenyl)vinyl]phenol, with bromopropane (1.5 equiv) in the presence of potassium carbonate (1 equiv) in acetone (1 mL per mmol of phenol). The 4-[(E)-2-(4-nitrophenyl)vinyl]phenol was synthesized by using a recent procedure previously described.[32]

mp: 114° C; IR (KBr): 536, 842, 963, 973, 1110, 1175, 1245, 1259, 1273, 1307, 1343, 1323, 1514, 1568, 1590, 1605, 2875, 2936, 2967 cm^{-1};^{1}H NMR (400 MHz, $CDCl_3$, δ, ppm): 1.05 (t, $J = 7.4$ Hz, 3H), 1.82 (sext, $J = 7.4$ Hz, $J = 6.6$ Hz, 2H), 3.96 (t, $J = 6.6$ Hz, 2H), 6.92 (d, $J = 8.4$ Hz, H_2, H_6), 7.00 (d, $J = 16.4$ Hz, $1H_{vinyl}$), 7.22 (d, $J = 16.4$ Hz, $1H_{vinyl}$), 7.48 (d, $J = 8.4$ Hz, H_3, H_5), 7.59 (d, $J = 8.8$ Hz, $H_{3'}$, $H_{5'}$), 8.20 (d, $J = 8.8$ Hz, $H_{2'}$, $H_{6'}$);^{13}C NMR (100.6 MHz, $CDCl_3$, δ, ppm): 10.5, 22.5, 69.6, 114.9 (2C), 123.9, 124.1 (2C), 126.5 (2C), 128.4 (2C), 128.7, 133.0, 144.3, 146.4, 159.8

9,9-Didecyl-N^2,N^7-bis{4-methoxyphenyl}-N^2,N^7-diphenyl-9H-fluoren-2,7-diamine (*DAF*). The synthesis and the characterization of **DAF** is described in reference.[33]

The solvents used for absorption and emission analysis are as follows: hexane (HEX), decane (DEC), butyl ether (BOE), ethyl ether (EOE), butyl acetate (BuAc), ethyl acetate (EtAc), butyl chloride (nBuCl), tetrahydrofuran (THF), dichloromethane (CH_2Cl_2), acetone (ACT), N,N-dimethylformamide (DMF), propionitrile (PPCN), propylene carbonate (PC), acetonitrile (ACN), ethanol (EtOH), methanol (MeOH). All the solvents employed were Aldrich or Fluka spectroscopic grade. The absorption and fluorescence of all solvents were checked for impurities and have been subtracted from the sample spectra. *N*-methyl diethanolamine (MDEA) were purchased from Aldrich. Polyethylene glycol diacrylate monomer (SR344, $M_w = 508$ g mol^{-1}) was provided by Sartomer.

2.2. General Techniques. The absorption measurements were carried out with a Perkin-Elmer Lambda 2 spectrometer. Steady-state fluorescence and phosphorescence spectra were collected from a FluoroMax-4 spectrofluorometer. Emission spectra are spectrally corrected, and fluorescence quantum yields include the correction due to solvent refractive index and were determined relative to quinine bisulfate in 0.05 molar sulfuric acid ($\Phi = 0.52$).[34]

The fluorescence lifetimes were measured by using a Nano LED emitting at 372 nm as an excitation source with a nano-led controller module, Fluorohub from IBH, operating at 1 MHz. The detection was based on an R928P type photomultiplier from Hamamatsu with high-sensitivity photon-counting mode. The decays were fitted with the iterative reconvolution method on the basis of the Marquardt/Levenberg algorithm.[35] Such a reconvolution technique allows an overall-time resolution down to 0.2 ns. The quality of the exponential fits was checked by using the reduced χ^2 (≤ 1.2).

Phosphorescence and steady-state anisotropy measurements were performed in ethanol at 77 K. The samples are placed in a 5 mm diameter quartz tube inside a Dewar filled with liquid nitrogen. Two Glan-Thompson polarizers are placed in the excitation and emission beams. The anisotropy r is determined as follows: $r = (I_{VV} - gI_{VH})/(I_{VV} + 2gI_{VH})$ with $g = (I_{HV})/(I_{HH})$, where I is the fluorescence intensity. The subscripts denote the orientation (horizontal H or vertical V) of the excitation and emission polarizers, respectively. g is an instrumental correction factor. The proper calibration of the setup was checked by using a recent standard method with rhodamine 101 in glycerol.[36]

The cyclic voltammetry experiments (performed by using a computer-controlled Princeton 263A potentiostat with a three-electrode single-compartment cell; a saturated calomel electrode in methanol used as a reference was placed in a separate compartment) were performed at 300 K, in Ar-degassed acetonitrile with a constant concentration (0.1 M) of n-Bu_4BF_4. Ferrocene was used as an internal reference.

Transient absorption experiments were carried out by laser flash photolysis at nanosecond time scale with an Edinburgh Analytical Instruments LP900 equipped with a 450 W pulsed Xe arc lamp, a Czerny-Turner monochromator, and a fast photomultiplier. The samples were irradiated with the third harmonic ($\lambda = 355$ nm, ~10 ns, 5 mJ per pulse) of a Nd/YAG Powerlite 9010 from Continuum. The sample concentration was adjusted to get an optical density of ~0.3 at the excitation wavelength and purged with nitrogen for 15 min prior to photophysical studies.

Quantum yields of trans→cis photoisomerization were carried out under irradiation at 372 nm with a laser diode from Cube type from Coherent. The progress of the reaction was monitored via UV−vis absorption spectra. The incident-light intensity was measured by the Aberchrome 540 actinometer dissolved in toluene.[37]

The 2PA measurements were performed with femtosecond mode-locked laser pulse by using a Ti:Sapphire laser (Spectra-Physics, Mai Tai: pulse duration, ~100 fs; repetition rate 80 MHz; wavelength range: 690−1020 nm). A relative two-photon induced-fluorescence method[17,38] was employed to measure the 2PA cross sections, δ. A 10^{-4} M solution of Coumarin 480 in methanol was used as the reference (r).[39] The value of δ for a sample (s) is given by

$$\delta_S = \frac{S_s \Phi_r \eta_r C_r}{S_r \Phi_S \eta_s C_s} \delta_r$$

where S is the detected two-photon induced fluorescence integral area, C is the concentration of the chromophores, and Φ is the fluorescence quantum yield of the chromophores. η is the collection efficiency of the experimental setup and accounts for the wavelength dependence of the detectors and optics as well as for the difference in refractive indices between the solvents

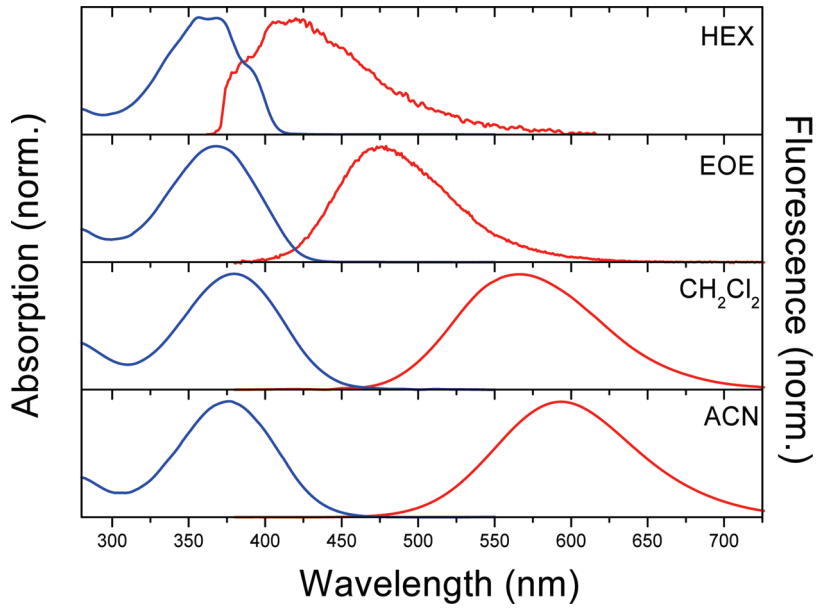

Figure 1. Normalized absorption and fluorescence spectra of **PNS** in solvents of different polarity.

TABLE 1: Spectroscopic Data of PNS at Room Temperature in Various Solvents

no.	solvent	λ_a^{max} (nm)[a]	λ_f^{max} (nm)[a]	$\Delta\nu_{Stokes}$ (cm^{-1})	Φ_f	$\Phi_{t\rightarrow c}$	τ, ns	k_f (10^7 s^{-1})	k_f/k_f^{SB}	k_{nr} (10^7 s^{-1})
1	HEX	357, 369	408, 420	4200	$<10^{-4}$	0.52	<0.2			
2	DEC	358, 372	408, 428	4570	$<10^{-4}$	0.51	<0.2			
3	BOE	367	451	5075	0.0005	0.32	<0.2			
4	EOE	368	476	6165	0.0005	0.42	<0.2			
5	BuAc	373	501	6850	0.0160	0.31	0.25	6.4	0.26	394
6	EtAc	373	521	7615	0.0400	0.30	0.92	4.3		104
7	nBuCl	371	506	7190	0.0280	0.27				
8	THF	375	515	7250	0.0520	0.24	1.0	5.2		94.8
9	CH_2Cl_2	379	566	8720	0.16	0.05	2.0	8.0	0.44	42.0
10	ACT	375	559	8780	0.22	0.05	2.8	7.9		27.9
11	DMF	383	581	8900	0.18	0.03	2.5	7.2		32.8
12	PPCN	375	572	9185	0.15	0.04	2.2	6.8		38.6
13	PC	379	594	9550	0.08	0.04	1.4	5.7		65.7
14	ACN	375	591	9750	0.09	0.03	1.5	6.0	0.40	60.7
15	MeOH	373				0.07	<0.2			
16	EtOH	374				0.10	<0.2			

[a] In case of double maxima, the main one is underlined and used for the solvatochromic plot.

in which the reference and sample compounds are dissolved. The measurements were conducted in a regime where the fluorescence signal showed a quadratic dependence on the intensity of the excitation beam, as expected for two-photon-induced emission. The collection of the two-photon-induced fluorescence signal was performed at the same detection wavelength ($\lambda_{exc} = 781$ nm) for coumarin 480 and compounds. The concentration of the solutions was in the range of $3-4 \times 10^{-4}$ M for compounds. The laser intensity was in the range of $0.2-2 \times 10^9$ W/cm^2. The experimental error on the reported cross section is 15−20%.

The one-photon polymerization was monitored in situ by real-time Fourier-transformed infrared spectroscopy with an AVATAR 360 FTIR spectrometer from Nicolet. A formulation of monomer containing the photoinitiator (0.5 wt%) and MDEA (5 wt%) is sandwiched between two polypropylene film (10 μm thick), deposited on a BaF_2 pellet and irradiated at 372 nm. The conversion rates are obtained from the disappearance of the progressive vinyl C=C stretching vibration band at 1630 cm^{-1}.

The two-photon polymerization was carried out by using similar formulations which are poured onto a glass slide and laminated with a cover glass. The same laser as the one used for the 2PA cross-section measurements was focused through a lens ($f = 5$ cm). The sample was placed on an X-step motorized stage controlled by a computer. The two-photon polymerized dots were recorded and dimensioned with a transmitted-light microscope.

ESR experiment was carried out with phenyl-*N*-*tert*-butylnitrone (PBN) as trap. A solution of *tert*-butyl benzene containing **PNS**, MDEA, PBN at 5×10^{-3}, 10^{-2}, and 0.1 M, respectively, is introduced into a cylindrical ESR tube and purged with argon for 15 min. ESR spectra were recorded with a X-band spectrometer (MS200 Magnettech) after irradiation of the sample by using a Hg−Xe Lamp (Hamamatsu, L8252, 150W) equipped with a long-pass filter ($\lambda > 360$ nm).

Semi empirical quantum chemical calculations were performed by using AM1 method (from HYPERCHEM package[40]).

3. Results and Discussion

3.1. Photophysical Feature of PNS. Figure 1 shows the normalized absorption and fluorescence spectra of **PNS** in various solvents of increasing polarity. The corresponding absorption and emission data are listed in Table 1. In the red-

energy side of the absorption spectrum, the chromophore exhibits an intensive band which is red-shifted upon increasing solvent polarity. The intensity of the last absorption is slightly increasing with ε_{MAX} of about 28900, 29300, and 29500 M^{-1} cm^{-1} in *n*-butylacetate, dichloromethane, and acetonitrile, respectively. However, the band shape is strongly affected by the nature of solvent, because, in non polar solvent, the last absorption band shows vibrational structuration, whereas, in medium and highly polar solvents, the structuration disappears, leading to a more Gaussian-shaped band. Figure 2 displays the excitation anisotropy spectrum of **PNS** in glassy matrix of ethanol at 77 K. The spectrum clearly exhibits a plateau in the 365−450 nm range with a constant value of ~0.32 ± 0.04. This plateau confirms the presence of a single electronic transition, the transition moment of which is roughly collinear to the transition moment at the absorption. Interestingly, a noticeable decrease of the anisotropy is observed below 360 nm, which indicates the presence of other transitions with distinctive electronic symmetry.

The fluorescence band of **PNS** shows a very strong solvatochromic red shift (Figure 1). In hexane, the fluorescence spectrum of **PNS** consists of a structured band which exhibits an approximate mirror−image relationship to the absorption spectrum. The corresponding Stokes shift has a low value of ~4200 cm^{-1}. However, in acetonitrile, **PNS** exhibits a broad, unstructured fluorescence band with a large Stokes shift of ~9750 cm^{-1}. This hints at a significant electronic or geometrical change between ground and excited state in polar solvent. Such a relaxation process can be evaluated by comparison of the fluorescence rate constant k_f with Strickler−Berg rate constant k_f^{SB} calculated from eq 1:[41]

$$k_f^{SB} = \frac{8\pi c 10^3 \ln 10}{N_L} n^2 \nu_f^3 \int \varepsilon(\nu_a) \mathrm{d}(\ln \nu_a) \qquad (1)$$

In this equation c, n, N_L, and ν_f correspond to the speed of light, the refractive index of the solvent, the Avogadro number, and the spectral position of the fluorescence maximum, respectively. The integrated band-absorption spectrum is proportional to the square of absorption transition moment as follows:[42,43]

$$\int \varepsilon(\nu_a) \mathrm{d}(\ln \nu_a) = \frac{8\pi^3 N_L n}{3hc10^3 \ln 10} M_a^2 \qquad (2)$$

The fluorescence electronic-transition dipole moment, M_f, can be derived from the fluorescence rate ($k_f = \Phi_f/\tau_f$) according to the eq 3:[44,45]

$$k_f = \frac{64\pi^4}{3h} n^3 \nu_f^3 M_f^2 \qquad (3)$$

The ratio between k_f and k_f^{SB} leads to the ratio of the squared fluorescence and absorption moments. If a value close to unity is obtained, it indicates that no change of the electronic or molecular structure occurs in S_1 state. However, in our case (see Table 1), k_f/k_f^{SB} largely deviates with values of ~0.44 in dichloromethane and ~0.40 in acetonitrile. Therefore, a strong electronic or conformational change between the absorption and fluorescence processes is clearly evidenced.

According to the considerable redshift of the fluorescence band with increasing solvent polarity, the emitting species should exhibit a strong charge-transfer character. The dipole moment at the excited state can thus be estimated from the Lippert−Mataga formalism.[46,47] If we only take into account the dipole−dipole interaction for the contribution of the solvent to the energy of the excited states (solvents inducing specific interactions are thus excluded), the dipole moment of the emitting excited state can be evaluated from the following equation:

$$\upsilon_{fluo} = -\frac{1}{4\pi\varepsilon_0} \frac{2\mu_e(\mu_e - \mu_g)}{hca^3} \Delta f + \text{const} \qquad (4)$$

μ_e is the excited-state dipole moment, and μ_g is the ground-state dipole moment. This latter parameter was derived from the full optimized geometrical structure of the chromophore by using AM1 method; the calculated dipole moment at ground state has a calculated value of ~7.3 D. Δf is the solvent-polarity parameter defined by $\Delta f = (\varepsilon - 1)/(2\varepsilon + 1) - (1/2)(n^2 - 1)/(2n^2 + 1)$ where ε is the relative permittivity, n is the refractive index of the solvent, h is the Planck constant, and c is the speed of light. The Onsager radius a defined as the solvent shell around the molecule was estimated to a value of ~7 Å. This value corresponds to 40% of the longest axis of the compound as suggested by Lippert[47] for nonspherical molecules. We also

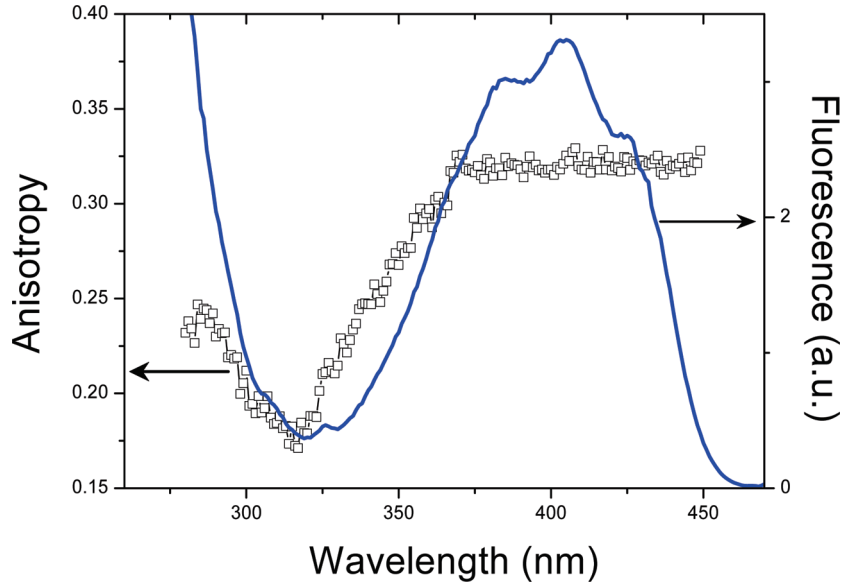

Figure 2. Fluorescence excitation spectrum and excitation anisotropy of **PNS** (squares) in glassy matrix of ethanol at 77 K (λ_{em} = 500 nm).

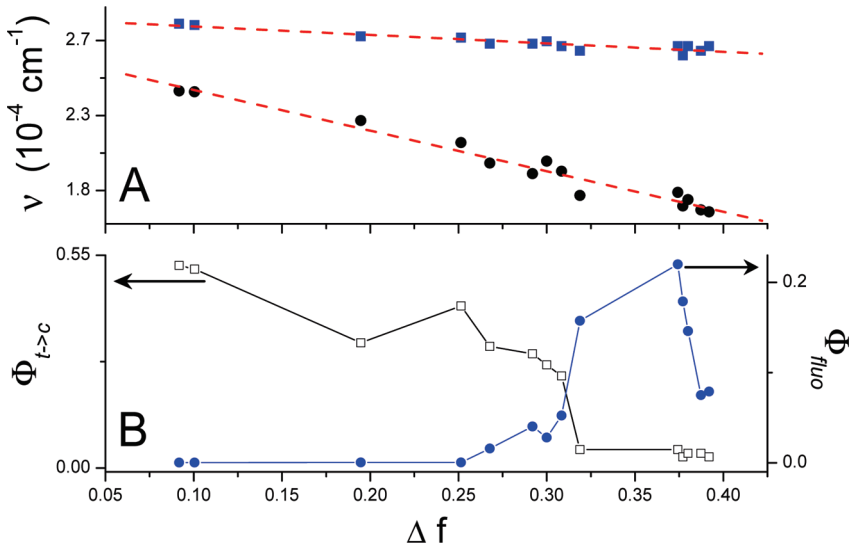

Figure 3. (A) Absorption (squares) and fluorescence (circles) maxima of **PNS** versus Δf. (B) Fluorescence quantum yield (circles) and trans→cis photoisomerization quantum yield (squares) as function of Δf.

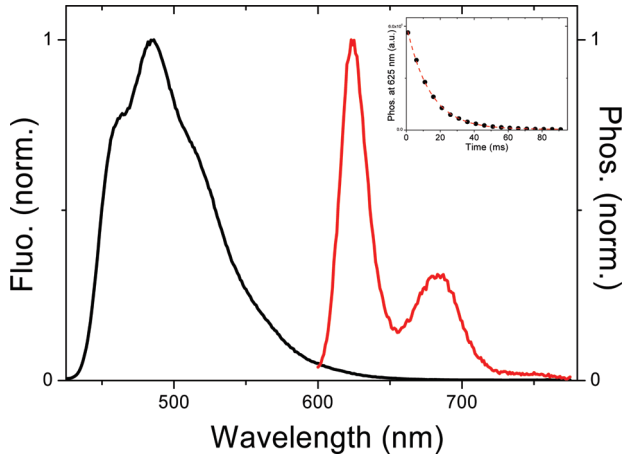

Figure 4. Normalized fluorescence and time-gated phosphorescence spectra of **PNS** in glassy matrix of ethanol (77 K). Inset: decay profile of the phosphorescence signal monitored at 630 nm.

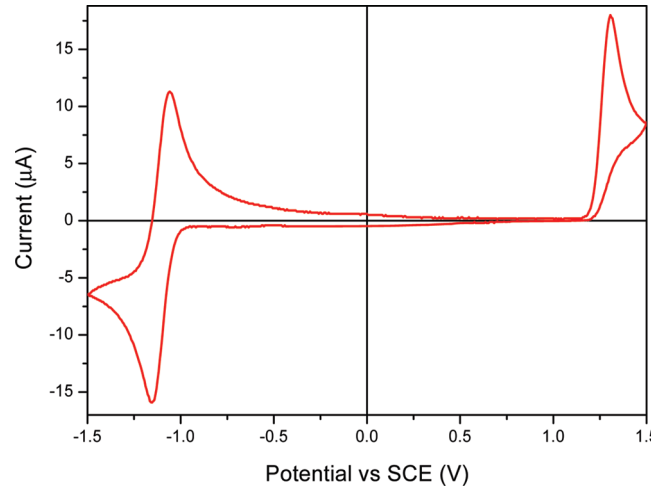

Figure 5. Cyclic voltamogramms of **PNS** in acetonitrile + $(n\text{-Bu})_4NPF_6$ (0.1 M) on platinum electrode at 200 mV s^{-1} (concentration of chromophore, 1.6×10^{-3} M).

assume that the dipole moment of the Franck−Condon ground state reached upon emission from the relaxed excited state is identical with the ground-state dipole moment μ_g. Figure 3A shows the plot of the maximum emission wavenumbers in function of their corresponding solvent-polarity parameter; the linear correlation exhibits a slope of about -25100 ± 1100 cm^{-1} which leads to a value of 33.1 ± 0.6 D for the excited dipole moment. This very large dipole moment, which is in the same range as those calculated for dimethylaminonitro (or cyano) stilbenes,[48–51] is consistent with the assignment of a TICT nature of the emitting state. The previous chemical quantum calculations relative to the excited-state properties of the 4-dimethylamino-4′-nitrostilbene[48,52] indicate that the excited chromophore undergoes a geometrical relaxation at S_1 surface from a planar LE to a perpendicular one which has the entire nitrophenyl moiety twisted about the central C−C bond ($\Theta_1 \approx 90°$, see Scheme 1). This twisted mechanism can be reasonably transposed to our case.

Figure 4 shows the emission spectrum of **PNS** in glassy matrix of ethanol. Although the fluorescence of **PNS** cannot be detected at room temperature, an intensive and structured band is observed in the 450−550 nm range. Moreover, in solid states, **PNS** undergoes a dramatic decrease of the Stokes shift with respect to that observed in equivalent polar solvent. This suggests that conformational change at the excited state is strongly hampered in glassy matrix. Figure 4 also shows the phosphorescence spectrum of **PNS**. The time-gated emission band shows a maximum at 625 nm, which leads to a low triplet energy of ∼1.98 eV. This spectrum exhibits a vibronic structure with a progression of several peaks. The frequency of the mode progression is about 1350 cm^{-1}, which nicely corresponds to the NO_2 symmetric stretching frequency.[53,54] According to the vibrational structuration of the phosphorescence and the short emission lifetime (i.e., 13.2 ms), the T_1 state of **PNS** clearly exhibits a strong $n\pi^*$ character.

The free energy associated to the photoinduced charge transfer at S_1 state (ΔG_{eT}) can be estimated according to the Rehm−Weller formalism:

$$\Delta G_{eT} = E_{ox} - E_{red} - E_{00} - C \qquad (5)$$

where E_{ox} and E_{red} correspond to the oxidation and reduction potentials of the donor and acceptor, respectively. E_{00} is the energy of the singlet excited state which has a value of ∼2.71 eV in acetonitrile. C is the Coulombic energy term characterizing the interaction of the radical ion pairs. In acetonitrile, this term is equal to 0.06 eV for a complete separation of one electron

SCHEME 2: Schematic Representation of States and Transitions Leading to the Deactivation of the Singlet LE in Solvents of Increasing Polarity: (A) Hexane, (B) Dichloromethane, and (C) Acetonitrile

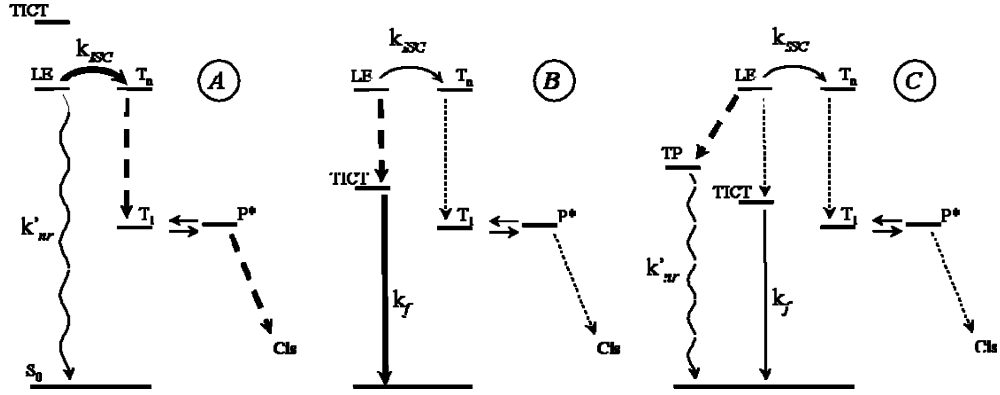

charge. Moreover, in the above equation, the value of $E_{ox} - E_{red}$ can be determined from cyclic voltammetry measurements. Figure 5 shows the voltammogram of **PNS** in acetonitrile containing 0.1 M of $(n\text{-Bu})_4NPF_6$; the cathodic part corresponds to the reversible reduction of 4-nitrophenyl moiety, and its half-wave potential has a value of about −1.11 V/SCE, perfectly comparable to the reduction potential of nitrobenzene.[55] At high potential, an irreversible oxidation wave is observed and should be ascribed to the formation of the radical cation centered in 4-propoxyphenyl fragment. The potential of the maximum oxidation wave is located at 1.34 V/SCE, which is clearly lower than that of anisole (1.65 V/SCE); such a difference suggests the involvement of the vinyl function in the stabilization of the radical cation. According to the cyclic voltammetry data, $E_{ox} - E_{red}$ is estimated to a value of 2.45 eV, which leads to a $\Delta G_{eT} = -0.32$ eV in acetonitrile. Therefore, the photoinduced intramolecular charge transfer from the 4-propoxyphenyl subunit to the 4-nitrophenyl moiety is thermodynamically allowed.

From the radiative rate constant (k_f) obtained for seven solvents of different polarity (Table 1), we can notice that k_f remains globally invariant. Therefore, the radiative deactivation of S_1 state should proceed from the TICT state. Conversely, the non-radiative rate constant (k_{nr}) is strongly dependent on solvent polarity with a non-monotonous evolution. A similar tendency is observed when considering the fluorescence quantum yield. Figure 3B shows Φ_f plotted versus Δf; we can clearly notice that Φ_f possesses a maximum for acetone and then decreases for highly polar solvent. This effect, which was also observed by Lapouyade et al.[48] for a series of donor nitrostilbenes, illustrates the role of the solvent polarity for the activation of multiple relaxation pathways at singlet state. In low- and non-polar solvent, the main non-radiative deactivation channel stems from an efficient intersystem crossing process (ISC). The presence of the NO_2 group should promote a considerable spin−orbit coupling, in accordance with the high Φ_{ISC} (∼0.9) measured for the 4-methoxy-4′-nitrostilbene[50] in cyclohexane. Moreover, Gegiou et al.[49] proposed that the population of T_1 state occurs through internal conversion from a T_n level which is approximately isoenergetic with S_1. The large energy gap measured between S_1 and T_1 (∼0.57 eV from Figure 4) corroborates the presence of high-lying T_n levels that should be implicated in the ISC process.

Figure 3B also shows the quantum yield of the trans→cis photoisomerization ($\Phi_{t\rightarrow c}$) as a function of Δf. A drastical decrease of $\Phi_{t\rightarrow c}$ is observed on going from apolar to polar solvent. Even though the direct trans→cis photoisomerization of **PNS** should constitute an alternative deactivation process at single state, it was extensively demonstrated that the main route for this photoreaction occurs via the T_1 level.[49,50,54,56–60] The photoreaction proceeds through a biradical twisted triplet state P* with a configuration perpendicular with respect to the C=C double bond.[61,62] According to this triplet mechanism, the photoisomerization reaction constitutes a minor channel for the deactivation of the S_1 state. Therefore, the decrease observed for $\Phi_{t\rightarrow c}$ can be either ascribed to a solvent dependency of the photoisomerization at triplet state or to a strong decrease of Φ_{ISC} upon increasing solvent polarity. From the evolution of Φ_{ISC} measured for 4-methoxy-4′-nitrostilbene[50] in solvents of different polarities, the latter assumption is clearly supported. For instance, it was observed that Φ_{ISC} is divided by a factor eight from cyclohexane to dimethylformamide. Hence, the fluorescence channel at S_1 state, in solvents of intermediate polarity, is promoted to the detriment of the intersystem crossing. This effect should be ascribed to a preferential stabilization of the emitting TICT state in polar solvent as illustrated in Scheme 2.

Finally, the progressive decrease of Φ_f at the high end of the solvent polarity scale indicates the occurrence of a third non-radiative deactivation channel. This new process has been assigned to the involvement of a so-called trap state[48] (TP) connected with the twisting of the nitro group from the planar LE. Such a conformational change occurs via another reaction coordinate (i.e., Θ_2 in Scheme 1) and produces a highly polar excited state which is non-emissive. In the same manner as the one previously observed, this TP should be strongly stabilized in high-polar solvents compared with the LE one. Consequently, the geometrical relaxation toward this low-lying state competes with that which produces the emitting one (Scheme 2). Hence, the photophysical behavior of **PNS** is strongly influenced by the nature of the solvent because of the presence of very high-polar excited states. This latter aspect obviously constitutes an essential requirement for a highly two-photon active chromophore.

3.2. 2PA Cross-Section Measurements. 2PA cross-section measurements have been carried out by using two-photon excited fluorescence (TPEF). The 2PA spectrum of **PNS** in acetonitrile is presented in Figure 6. The 2PA spectrum exhibits a broad structured band localized in the 700−900 nm range and a maximum intensity at 800 nm. It is worth noting that the apparent vibronic structure of the 2PA spectrum resembles that obtained for other nitrostilbene derivatives.[63,64] The absorption cross section at the maximum intensity exhibits a value of ∼220 ± 15 GM. This value is in the same range as that obtained for the 4-dimethylamino-4′-nitrostilbene.[65,66] In a first approximation, the major contribution for the 2PA cross section of the asymmetrical donor−acceptor polyenes originates from the so-called dipolar term that involves the difference between the dipole moments in the ground state and in the lowest charge-

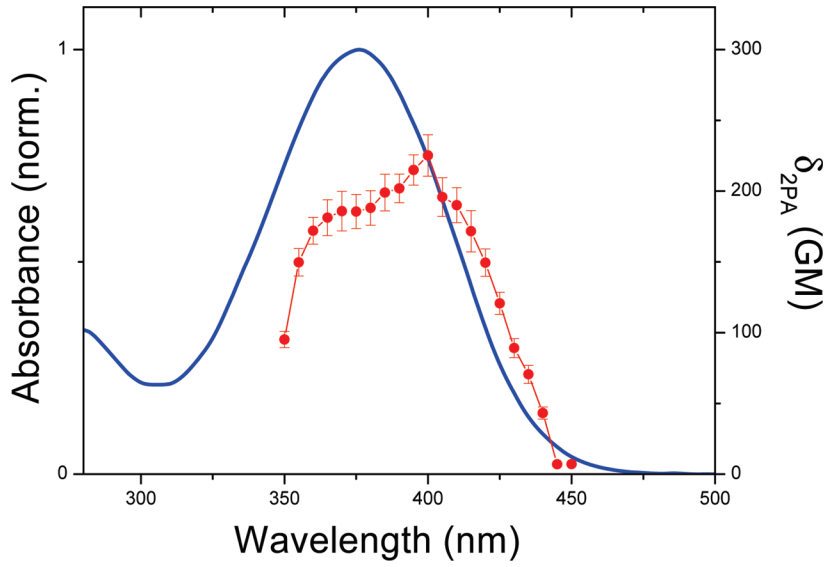

Figure 6. Linear absorption and 2PA (circles) spectra of **PNS** in acetonitrile.

transfer excited state. In this two-state model, δ can be approximated by the following relation:[21,67]

$$\delta \propto \frac{M_{ge}^2 \Delta\mu_{ge}^2}{E_{ge}^2} \quad (6)$$

E_{ge} is the transition energy from the ground state to the state e. M_{ge}, which represents the corresponding transition dipole moments, is calculated from the eq 2 and has a value of ~7.6 D. $\Delta\mu_{ge}$ is the dipole-moment change. This parameter can be estimated from the solvatochromic equation for absorption:[46,47]

$$\upsilon_{abs} = -\frac{1}{4\pi\varepsilon_0}\frac{2\mu_g\Delta\mu_{ge}}{hca^3}\Delta f + \text{const} \quad (7)$$

Here, the formalism is exactly the same as that used in eq 4 except that the excited state reached upon excitation corresponds to the Franck−Condon one. The plot of the maximum absorption wavenumbers versus Δf is displayed in Figure 3A. The linear correlation exhibits a slope of -5100 ± 500 cm^{-1} which leads to a $\Delta\mu_{ge}$ of ~23 ± 3 D. This large value points to a relatively strong dipole moment of the Franck−Condon excited state (around 16 D). Hence, the right-hand term of eq 6 has a value of ~2800 D^4 eV^{-2}. From the linear correlation obtained by Antonov et al.[66] for a series of push−pull nitrostilbene derivatives, our estimate is in good agreement with the δ that can be extrapolated (i.e., 200 GM). Even though the two-state model leads to an acceptable value of δ, it fails to explain the unexpected red shift observed when going from the linear to the nonlinear absorption spectra (the shift is particularly pronounced with a value of 0.10 eV). Such an effect, which was also clearly observed for the 4-dimethylamino-4′-nitrostilbene,[65,68] has been rationalized by Beljonne et al.[68] who suggested the involvement of the two-photon allowed S_1 and S_2 states. In this proposed three-state model, the vibronic structure was implemented in the calculation of the Franck−Condon factors leading to the determination of the different distributions of the intensities associated with the various vibronic features in the 2PA spectrum. Such a vibronic coupling within Franck−Condon approximation partly explains the observed red shift.

3.3. One- and Two-Photoinitiating Ability of PNS. From the photophysical analysis of **PNS**, we can infer that, in low-polar medium, the deactivation of the excited chromophore mainly proceeds through intersystem crossing. Moreover, the phosphorescence spectrum indicates that the triplet state exhibits a markedly nπ* character which undoubtedly constitutes a key advantage for the hydrogen-abstraction reaction. Therefore, a large production of reactive T_1 species should lead to an efficient free-radical photoinitiating route. To compare the one- and two-photon polymerization of **PNS**, we used a 2,7 diaminofluorene derivative (**DAF**) which has already been employed as one- and two-photon photonitiator.[23,27,33,69] **DAF** is absorbing in the same spectral region as **PNS** with a maximum absorption band centered at 375 nm in acetonitrile (ε_{MAX} = 29800 M^{-1} cm^{-1}). The 2PA cross section of **DAF** at 750 nm has a value of ~150 ± 15 GM in acetonitrile, whereas **PNS** has a δ of ~180 ± 15 GM.

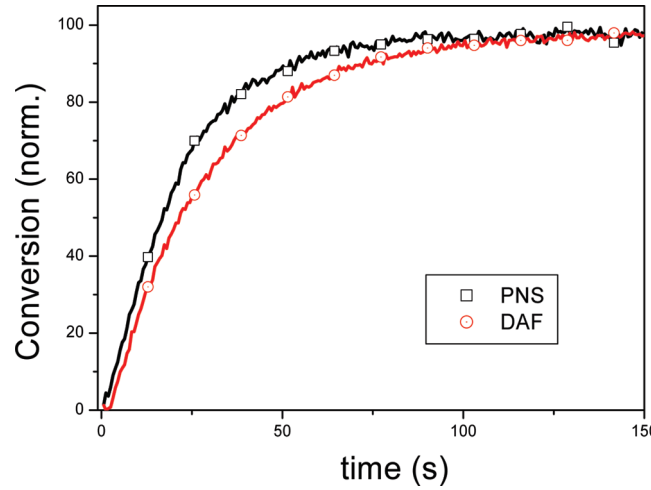

Figure 7. Conversion vs time curves for photopolymerization of diacrylate monomer. Photoinitiating systems: **PNS**/ MDEA, 0.5 wt%/5 wt% (squares); **DAF**/ MDEA, 0.5 wt%/5 wt% (circles).

Figure 7 shows the conversion rate of acrylate double bonds upon irradiation at 372 nm of two formulations containing the chromophores dissolved in diacrylate monomer with 5 wt% of MDEA. This latter component is used as hydrogen-donor reactant. In both cases, a final conversion of 95% is reached after 100 s irradiation. Moreover, the similar value for the initial rates of photopolymerization indicates that both chromophores exhibit the same reactivity under our irradiation condition (i.e.,

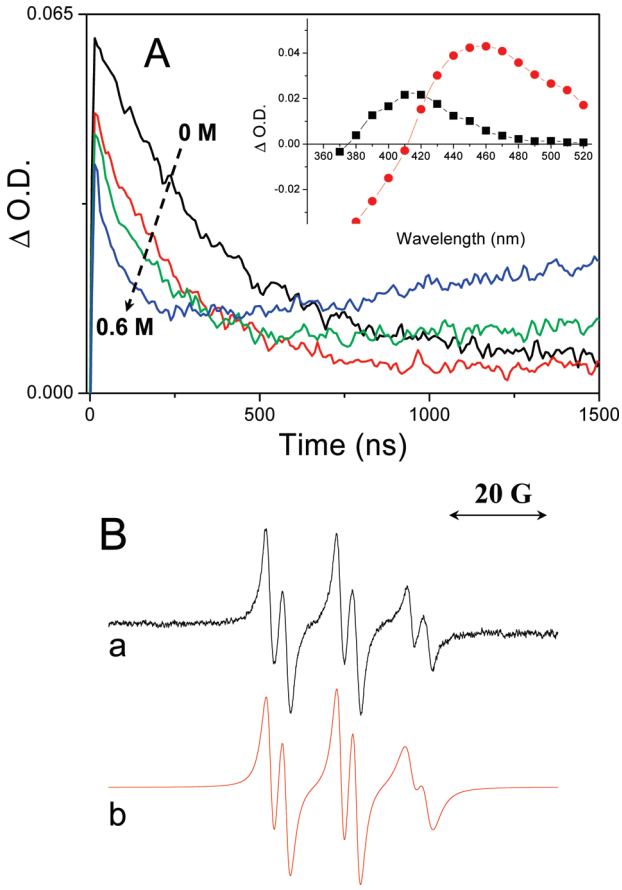

Figure 8. (A) Evolution of the transient-absorption time profile of **PNS** at 460 nm upon addition of MDEA (solvent: acetonitrile, [PNS] = 2×10^{-5} M). Inset: Transient absorption spectra of **PNS** (2×10^{-5} M) mixed with MDEA (0.6 M) recorded at 60 ns (squares) and 3 μs (circles) after 355 nm laser pulse excitation. (B) (a) ESR spectrum of spin trap adduct generated in the ^{3}**PNS**/ MDEA system in presence of PBN. (solvent: *tert*-butyl benzene, [**PNS**] = 5×10^{-3} M, [MDEA] = 10^{-2} M, [PBN] = 0.1 M). (b) Simulated spectrum.

P $\approx$ 5 mW.cm^{-2}). It is to be noted that, at low-power irradiation (irradiance < 4 mW.cm^{-2}.), an induction time is observed at the first steps of the conversion-rate profile for the formulation with **DAF**. Such an effect is not observed with **PNS**. This hints at the very high oxygen sensitivity of the triplet state of **DAF** (^{3}**DAF**). From transient-absorption measurements, we have previously measured that the quenching rate of ^{3}**DAF** by oxygen exhibits a very high value of $\sim 1.6 \times 10^{10}$ M^{-1} s^{-1} in acetonitrile, which suggests a diffusion-controlled reaction.[33] Moreover, the photoinitiating process upon excitation of **DAF** is assumed to proceed through an electron transfer from ^{3}**DAF** to acrylate monomer which produces a radical cation that is subsequently used as hydrogen abstractor toward MDEA. In the case of **PNS**, the triplet states can directly react with MDEA, as illustrated by the evolution of the transient -absorption time profile of **PNS** upon addition of the amine in Figure 8A. First, it is worth noting that this transient can be confidently ascribed to the triplet of **PNS** (^{3}**PNS**), in good agreement with the results of Görner et al.[56] The T_1-T_n spectrum of **PNS** consists of a broadband located in the 410−550 nm range (inset Figure 8A). The kinetic decay follows a first-order kinetics, with a lifetime of ~350 ns. This short value stems from a rapid equilibrium at the triplet excited level between the trans configuration and the intermediate P* species (see Scheme 2). Moreover, this transient is quenched by oxygen with a rate of $\sim 1.3 \times 10^9$ M^{-1} s^{-1}. This value, which is 10 times lower than that obtained for **DAF**, corroborates the absence of induction time for the formulation with **PNS** during photopolymerization. From Figure 8A, we can observe that the gradual addition of MDEA leads to a progressive quenching of ^{3}**PNS**. The bimolecular quenching rate constant of ^{3}**PNS** by MDEA (k_q) can be determined from the dependence of the pseudofirst-order decay of the triplet dye on the concentration of MDEA according to the eq 7:

$$k_{obs} = k_0 + k_q[\text{MDEA}] \quad (7a)$$

Under this condition, the bimolecular quenching rate exhibits a value of $\sim 3.9 \times 10^6$ M^{-1} s^{-1}. Moreover, the progressive shortening of the triplet is accompanied by the growth of a long time component at the limit of the time profile. The corresponding transient-absorption spectrum consists of a single band centered at 420 nm. Because the transient signal was not observed for the oxygen-saturated solution, the transient species is assumed to be produced from the triplet state. This spectrum is markedly similar to that of the anion radical of the 4-methoxy-4′-nitrostilbene.[70] Hence, we suggest the occurrence of a photoinduced electron transfer from MDEA to ^{3}**PNS** leading to the formation of the radical anion. However, this electron-transfer process should constitute a minor deactivation pathway for ^{3}**PNS** according to the very low value of k_q in acetonitrile. Figure 8B shows the ESR spectrum obtained in the spin-trapping experiment of the radical generated from the ^{3}**PNS**/MDEA system in presence of PBN. The fit of the corresponding signal leads to nitrogen and hydrogen hyperfine splitting constants of ~1.51 and ~0.33 mT, respectively, in very good agreement[71] with the signal of a spin trap adduct formed with an α-aminoalkyl radical. Hence, the main product consecutive to the quenching of ^{3}**PNS** by MDEA is the α-aminoalkyl radical of MDEA. It is to be noted that the complementary monohydronitro radical product was not detected; this should be ascribed to the short-lived character of the species because of a very efficient radical−radical recombination[72] and/or a possible intramolecular-rearrangement mechanism[73,74] leading to the production of a phenol derivative and a released nitric oxide radical which is not trapped by PBN. Hence, **PNS** appears as a good hydrogen-abstractor photoreactant. In conjunction with a remarkable 2PA absorption property, **PNS** should constitute an efficient two-photon initiator for free radical photopolymerization. To demonstrate the 2PA polymerization ability of **PNS**, the fabrication of microdots was carried out by simply focusing the femtosecond pulse laser beam with a lens (f = 50 cm) into a diacrylate formulation with **PNS** and MDEA. Figure 9A shows the micrograph of the polymerized microstructures obtained upon excitation at 750 nm. Circular structures with an average radius of 15 ± 0.5 μm are obtained after 10 s laser exposure at 30 mW. The presence of MDEA as hydrogen donor is necessary, otherwise the two-photon polymerization is not observed. An equivalent formulation containing **DAF** at the same concentration as that prepared with **PNS** is used as a reference system; the corresponding microdots obtained under the same excitation condition are shown in Figure 9B. In this case, the polymer structures are clearly smaller, with an average radius of ~6 ± 0.5 μm. If we maintain the incident laser power at 30 mW, it should be noted that the two-photon polymerization for the reference formulation is not observed below an exposure time of 5 s, whereas the resin with **PNS** still leads to the appearance of microdots with mean radius of 11 ± 0.5 μm. Therefore, the two-photon initiation efficiency appears markedly superior for the **PNS** system and indicates that this photoinitiator should exhibit a lower two-photon polymerization threshold energy (E_{th}) as compared with **DAF** system. E_{th}, which is defined as the local absorbed-energy density below which the polymer is not obtained,[26] can be evaluated from point-by-point exposure experiments.[26,69,75,76] By assuming that the incident laser intensity presents a Gaussian profile in the

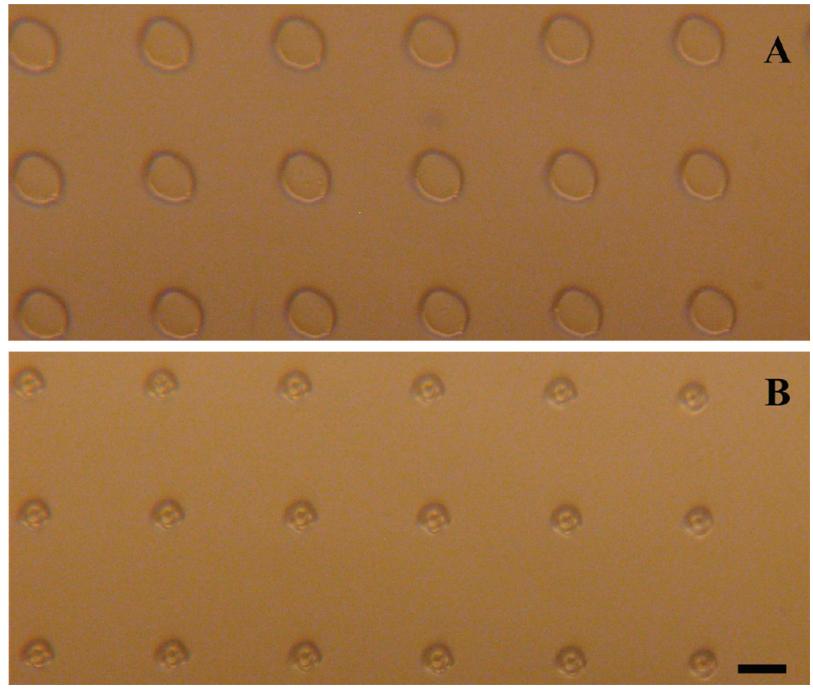

Figure 9. Two-photon polymerization voxels fabricated with femtosecond-laser direct writing by 2PA photopolymerization (scale bar, 30 μm; λ_{exc} = 750 nm; average power, 30 mW; exposure time, 10s). Diacrylate formulations with (A) **PNS**/MDEA, 0.5 wt%/5 wt% and (B) **DAF**/MDEA, 1.5 wt%/5 wt%.

focal plan and that the diffusion lengths of the reactive species are negligible in comparison with the size of the photopolymerized structures, the dependence of the voxel radius on the time-averaged incident power, $\langle P(t)\rangle$, for a fixed exposure time can be expressed as follows:[76]

$$r = \omega_0 \sqrt{2\ln \frac{\langle P\rangle}{\langle P\rangle_{\min}}} \tag{8}$$

ω_0 corresponds to the lateral width of the laser intensity at the focal plane and $\langle P(t)\rangle_{\min}$ is the minimum power necessary for two-photon polymerization. The threshold energy (E_{th}) is finally derived from $\langle P(t)\rangle_{\min}$ according to:

$$E_{th} = KN_i\delta\langle P\rangle^2_{\min} \tag{9}$$

K is a parameter which implies all the photonic conditions (exposure time, pulse shape parameter, laser temporal pulse width, and repetition rate of the laser). N_i and δ are the number density of the photoinitiator and the 2PA cross section, respectively. Figure 10 displays the radius of the polymer dots as a function of the incident power. The least-squares analysis of experimental data yields values for $\langle P(t)\rangle_{\min}$ of 11.3.mW for **PNS** and of 24.5 mW for **DAF**. Consequently, the ratio of the threshold energies between **PNS** and **DAF** exhibits a value of 0.26. Hence, we have clear improvement of the two-photon polymerization efficiency for **PNS**. Such an effect should be ascribable to the higher oxygen sensitivity of the triplet excited **DAF**. This effect, which was previously illustrated by the occurrence of an induction time at the initial step of the one-photon polymerization, appears as the main competing process for two-photon polymerization. This is also consistent with local effect of the oxygen inhibition leading to an adding contribution to the threshold energy of the two-photon polymerization.

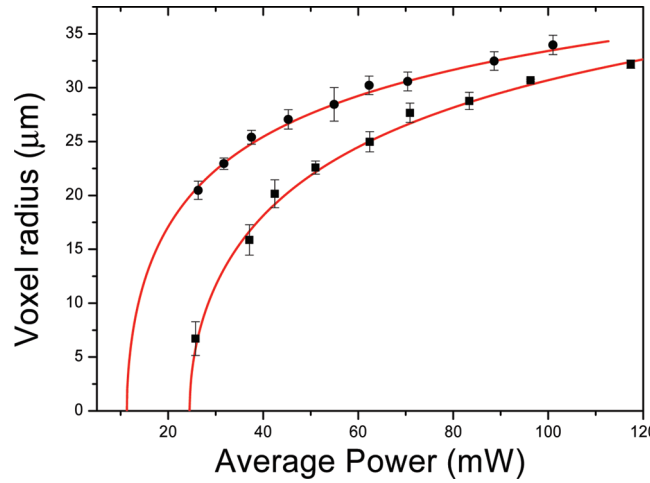

Figure 10. Variation of the polymerized voxel radius as a function of the incident average power (circles, **PNS**; squares, **DAF**; time exposure, 20s). The solid line corresponds to the best fit data obtained by using eq 8.

4. Conclusion

We have characterized the photophysical properties of the *trans*-4-propoxy-4′-nitrostilbene (**PNS**). The fluorescence, ISC, and trans−cis photochemical isomerization are strongly dependent on the polarity of the solvent which governs the sequential activation of multiple relaxation pathways at the singlet LE. In low -polar solvent, the planar LE mainly undergoes an efficient ISC to the triplet manifold from which the trans−cis photoisomerization occurs by rotation about the C═C double bond. The lowest triplet state which exhibits an nπ^* character is remarkably reactive toward aliphatic amine which undergoes a hydrogen-abstraction reaction and leads to the efficient production of α-aminoalkyl radicals. Therefore, **PNS** constitutes a good photoinitiating system for free-radical polymerization. However, on going from low-polar to high-polar solvents, the relaxation process at S_1 state induces a clear switcon of the fluorescence of **PNS** to the detriment of ISC and trans−cis photoisomerization. The LE relaxes directly to a highly polar TICT state derived by twisting of the entire nitrophenyl moiety. Further increase of the polarity (as for acetonitrile) opens

a new non-radiative channel whereby the nitro group is twisted. Because of the photoinduced charge transfer occurring in this donor-conjugated bridge acceptor system, **PNS** exhibits a sizable 2PA spectrum in the 700−900 nm region with $\delta \approx 180 \pm 15$ GM at 750 nm, which is in the same range as that obtained for **DAF**. This later system is used as reference for two-photopolymerization. According to the point-by-point exposure results, **PNS** exhibits a four-times lower threshold energy as compared with **DAF**. Hence, a substantial improvement of the two-photon polymerization efficiency for this class of D−π−A system was demonstrated.

References and Notes

(1) Ehrlich, J. E.; Wu, W. L.; Lee, Y. L.; Hu, Z. Y.; Rockel, H.; Marder, S. R.; Perry, J. W. *Opt. Lett.* **1997**, *22*, 1843.

(2) Morel, Y.; Irimia, A.; Najechalski, P.; Kervella, Y.; Stephan, O.; Baldeck, P. L.; Andraud, C. *J. Chem. Phys.* **2001**, *114*, 5391.

(3) Caylor, C. L.; Dobrianov, I.; Kimmer, C.; Thorne, R. E.; Zipfel, W.; Webb, W. W. *Phys. Rev. E* **1999**, *59*, 3831.

(4) Köhler, R. H.; Cao, J.; Zipfel, W. R.; Webb, W. W.; Hanson, M. R. *Science* **1997**, *276*, 2039.

(5) Miller, M. J.; Hei, S. H.; Parker, I.; Cahalan, M. D. *Science* **2002**, *296*, 1869.

(6) Denk, W.; Strickler, J. H.; Webb, W. *Science* **1990**, *248*, 73.

(7) Zhou, W. H.; Kuebler, S. M.; Braun, K. L.; Yu, T. Y.; Cammack, J. K.; Ober, C. K.; Perry, J. W.; Marder, S. R. *Science* **2002**, *296*, 1106.

(8) Kawata, S.; Sun, H.-B.; Tanaka, T.; Takada, K. *Nature* **2001**, *412*, 697.

(9) Maruo, S.; Nakamura, O.; Kawata, S. *Opt. Lett.* **1997**, *22*, 132–134.

(10) Sun, H.-B.; Kawata, S. *Two-Photon Photopolymerization and 3D Lithographic Microfabrication*; Springer-Verlag: Berlin, 2004; Vol. 170.

(11) Cumpston, B. H.; Ananthavel, S. P.; Barlow, S.; Dyer, D. L.; Ehrlich, J. E.; Erskine, L. L.; Heika, A. A.; Kuebler, S. M.; Lee, I.-Y. S.; McCord-Maughon, D.; Qin, J.; Röckel, H.; Rumi, M.; Wu, X.-L.; Marder, S. R.; Perry, J. W. *Nature* **1999**, *398*, 51–54.

(12) Kanis, D. R.; Ratner, M. A.; Marks, T. J. *Chem. Rev.* **1994**, *94*, 195.

(13) Marder, S. R.; Beratan, D. N.; Cheng, L. T. *Science* **1991**, *252*, 103.

(14) Kim, O.-K.; Lee, K.-S.; Woo, H. Y.; Kim, K.-S.; He, G. S.; Swiatkiewicz, J.; Prasad, P. N. *Chem. Mater.* **2000**, 284–286.

(15) Reinhardt, B. A.; Brott, L. L.; Clarson, S. J.; Dillard, A. G.; Bhatt, J. C.; Kannan, R.; Yuan, L.; He, G. S.; Prasad, P. N. *Chem. Mater.* **1998**, *10*, 1863–1874.

(16) Chung, S.-J.; Rumi, M.; Alain, V.; Barlow, S.; Perry, J. W.; Marder, S. R. *J. Am. Chem. Soc.* **2005**, *127*, 10844–10845.

(17) Rumi, M.; Ehrlich, J. E.; Heikal, A.; Perry, J. W.; Barlow, S.; Hu, Z. Y.; McCord-Maughon, D.; Parker, T. C.; Rockel, H.; Thayumanavan, S.; Marder, S. R.; Beljonne, D.; Brédas, J. L. *J. Am. Chem. Soc.* **2000**, *122*, 9500.

(18) He, G. S.; Tan, L.-S.; Zheng, Q.; Prasad, P. N. *Chem. Rev.* **2008**, *108*, 1245–1330.

(19) Bhaskar, A.; Ramakrishna, G.; Lu, Z.; Twieg, R.; Hales, J. M.; Hagan, D. J.; Stryland, E. V.; Goodson, T. *J. Am. Chem. Soc.* **2006**, *128*, 11840–11849.

(20) Brousmiche, D. W.; Serin, J. M.; Fréchet, J. M. J.; He, G. S.; Lin, T.-C.; Chung, S. J.; Prasad, P. N. *J. Am. Chem. Soc.* **2003**, *125*, 1448–1449.

(21) Beljonne, D.; Wenseleers, W.; Zojer, E.; Shuai, Z.; Vogel, H.; Pond, S. J. K.; Perry, J. W.; Marder, S. R.; Brédas, J. L. *Adv. Funct. Mater.* **2002**, *12*, 631.

(22) Chung, S. J.; Kim, K. S.; Lin, T. C.; He, G. S.; Swiatkiewicz, J.; Prasad, P. N. *J. Phys. Chem. B* **1999**, *103*, 10741.

(23) Jin, M.; Malval, J. P.; Versace, D. L.; Morlet-Savary, F.; Chaumeil, H.; Defoin, A.; Allonas, X.; Fouassier, J. P. *Chem. Comm.* **2008**, *48*, 6540–6542.

(24) Belfield, K. D.; Ren, X.; Stryland, E. W. V.; Hagan, D. J.; Dubikovsky, V.; Miesak, E. J. *J. Am. Chem. Soc.* **2000**, *122*, 1217–1218.

(25) Kuebler, S. M.; Braun, K. L.; Zhou, W.; Cammack, J. K.; Yu, T.; Ober, C. K.; Marder, S. R.; Perry, J. W. *J. Photochem. Photobio. A: Chem.* **2003**, *158*, 163–170.

(26) Martineau, C.; Lemercier, G.; Andraud, C.; Wang, I.; Bouriau, M.; Baldeck, P. L. *Synth. Met.* **2003**, *138*, 353–356.

(27) Martineau, C.; Anémian, R.; Andraud, C; W, I.; Bouriau, M.; Baldeck, P. L. *Chem.Phys.Lett.* **2002**, *362*, 291–295.

(28) Belfield, K. D.; Schafer, K. J.; Liu, Y.; Liu, J.; Ren, X.; Stryland, E. W. V. *J. Phys. Org. Chem.* **2000**, *13*, 837–849.

(29) Wu, J. Q.; Beranek, I.; Fischer, H. *Helv. Chim. Acta* **1995**, *78*, 194.

(30) Fischer, H.; Radom, L. *Angew. Chem., Int. Ed.* **2001**, *40*, 1340–1371.

(31) Turro, N. J. *Modern Molecular Photochemistry*; University Science Books: Sausalito, 1991.

(32) Diemer, V.; Chaumeil, H.; Defoin, A.; Carré, C. *Synthesis* **2007**, *21*, 3333–3338.

(33) Balan, L.; Jin, M.; Malval, J. P.; Chaumeil, H.; Defoin, A.; Vidal, L. *Macromolecules* **2008**, *41*, 9359–9365.

(34) Meech, R.; Phillips, D. *J. Photochem.* **1983**, *23*, 193–217.

(35) Connor, D. V.; Phillips, D. *Time correlated single photon counting*, Academic Press: London, 1984.

(36) Prazeres, T. J. V.; Fedorov, A.; Barbosa, S. P.; Martinho, J. M. G.; Berberan-Santos, M. r. N. *J. Phys. Chem. A* **2008**, *112*, 5034–5039.

(37) Heller, H. G.; Lagan, J. R. *J. Chem. Soc., Perkin. Trans.* **1981**, *2*, 341.

(38) Xu, C.; Webb, W. W. *J. Opt. Soc. Am. B* **1996**, *13*, 481–491.

(39) Fisher, W. G.; Wachter, E. A.; Lytle, F. E.; Armas, M.; Seaton, C. *Appl. Spectrosc.* **1998**, *52*, 536–545.

(40) *HYPERCHEM*, version 7.03; Hypercube, Inc.: Gainesville, FL, 2002.

(41) Strickler, S. J.; Berg, R. A. *J. Chem. Phys.* **1962**, *37*, 814.

(42) Berlman, I. B.; Steingraber, O. J. *J. Chem. Phys.* **1965**, *43*, 2140.

(43) Berlman, I. B. *J. Chem. Phys.* **1970**, *52*, 5616.

(44) Birks, J. B. *Photophysics of Aromatic Molecules*; Wiley-Interscience: New York, 1970.

(45) Maus, M.; Rettig, W.; Bonafoux, D.; Lapouyade, R. *J. Phys. Chem. A* **1999**, *103*, 3388–3401.

(46) Mataga, N.; Kaifu, Y.; Koizumi, M. *Bull. Chem. Soc. Jpn.* **1955**, *28*, 690.

(47) Lippert, E. *Z. Naturforsch.* **1955**, *10a*, 541.

(48) Lapouyade, R.; Kuhn, A.; Letard, J. F.; Rettig, W. *Chem. Phys. Lett.* **1993**, *208*, 48–58.

(49) Gegiou, D.; Muszkat, K. A.; Fischer, E. *J. Am. Chem. Soc.* **1968**, *90*, 3097–3918.

(50) Gurzadyan, G.; Görner, H. *Chem. Phys. Lett.* **2000**, *319*, 164–172.

(51) Lippert, E. *Elektrochem. Angew. Phys. Chem.* **1957**, *61*, 962.

(52) Farztdinov, V. M.; Ernsting, N. P. *Chem. Phys.* **2002**, *277*, 257–270.

(53) Epstein, L. M.; Shubina, E. S.; Ashkinadze, L. D.; Kazitsyna, L. *Spectrochim. Act.* **1982**, *38A*, 317–322.

(54) Görner, H. *J. Phys. Chem.* **1989**, *93*, 1926–1832.

(55) Leventis, N.; Dass, A. *J. Am. Chem. Soc.* **2005**, *127*, 4988–4989.

(56) Görner, H.; Schulte-Frohlinde, D. *J. Phys. Chem.* **1978**, *82*, 2653–2659.

(57) Bent, D. V.; Schulte-Frohlinde, D. *J. Phys. Chem.* **1974**, *78*, 446–450.

(58) Gruen, H.; Görner, H. *J. Phys. Chem.* **1989**, *93*, 7144–7152.

(59) Görner, H. *J. Photochem. Photobio. A: Chem.* **1987**, *40*, 325–339.

(60) Görner, H.; Schulte-Frohlinde, D. *J. Photochem.* **1978**, *8*, 91–102.

(61) Papper, V.; Pines, D.; Likhtenshtein, G.; Pines, E. *J. Photochem. Photobio. A: Chem.* **1997**, *111*, 87–96.

(62) Waldeck, D. H. *Chem. Rev.* **1991**, *91*, 415–436.

(63) Stellacci, F.; Bauer, C. A.; Meyer-Friedrichsen, T.; Wenseleers, W.; Marder, S. R.; Perry, J. W. *J. Am. Chem. Soc.* **2003**, *125*, 328–329.

(64) Beljonne, D.; Brédas, J. L.; Cha, M.; Torruellas, W. E.; Stegeman, G. I.; Hofstraat, J. W.; Horsthuis, W. H. G.; Möhlmann, G. R. *J. Chem. Phys.* **1995**, *103*, 7834–7843.

(65) Delysse, S.; Raimond, P.; Nunzi, J. M. *Chem. Phys. Lett.* **1997**, *219*, 341–351.

(66) Antonov, L.; Kamada, K.; Ohta, K.; Kamounah, F. S. *Phys. Chem. Chem. Phys.* **2003**, *5*, 1193–1197.

(67) Kogej, T.; Beljonne, D.; Meyers, F.; Perry, J. W.; Marder, S. R.; Bredas, J. L. *Chem. Phys. Lett.* **1998**, *298*, 1–6.

(68) Beljonne, D.; Brédas, J. L.; Cha, M.; Torruellas, W. E.; Stegeman, G. I.; Hofstraat, J. W.; Horsthuis, W. H. G.; Möhlmann, G. R. *J. Chem. Phys.* **1995**, *103*, 7834–7843.

(69) Lemercier, G.; Mulatier, J. C.; Martineau, C.; Anémian, R.; Andraud, C.; Wang, I.; Stephan, O.; Amari, N.; Baldeck, P. L. C.R. *Chimie* **2005**, *8*, 1308–1316.

(70) Görner, H.; Schulte-Frohlinde, D. *Chem. Phys. Lett.* **1986**, *124*, 321–325.

(71) Kotake, Y.; Kuwata, K. *Bull. Chem. Soc. Jpn.* **1981**, *54*, 394–398.

(72) Sutcliffe, L. H. *J. Chem. Soc., Perkin. Trans. 1* **1985**, *81*, 1467–1470.

(73) Hishikawa, K.; Kakagawa, H.; Furuta, T.; Fukuhara, K.; Tsumoto, H.; Suzuki, T.; Miyata, N. *J. Am. Chem. Soc.* **2009**, *131*, 7488–7489.

(74) Fukuhara, K.; Kurihara, M.; Miyata, N. *J. Am. Chem. Soc.* **2001**, *123*, 8662–8666.

(75) Lee, K.-S.; Yang, D.-Y.; Park, S. H.; Kim, R. H. *Polym. Adv. Technol.* **2006**, *17*, 72–82.

(76) Pruzinsky, S. A.; Braun, V. *Adv. Funct. Mater.* **2005**, *15*, 1995–2004.

JP9075977